CO-DIFFUSED APCVD BORON REAR EMITTER WITH SELECTIVELY ETCHED-BACK FSF FOR INDUSTRIAL N-TYPE SI SOLAR CELLS

Yvonne Schiele[1], Felix Book[1], Carsten Demberger[2], Kaiyun Jiang[2], Giso Hahn[1]
[1] University of Konstanz, Department of Physics, P.O. Box 676, 78457 Konstanz, Germany
[2] Gebr. SCHMID GmbH, Robert-Bosch-Str. 32-36, 72250 Freudenstadt, Germany
Phone: +49 (0) 7531 88 4995, Fax: +49 (0) 7531 88 3895, Email: Yvonne.Schiele@uni-konstanz.de

ABSTRACT: The employment of a B-doped atmospheric pressure chemical vapor deposited (inline belt APCVD) borosilicate glass is an elegant technology for industrially realizing a p^+ emitter. By drive-in of B and a subsequent $POCl_3$ co-diffusion, p^+ emitter and n^+ front surface field (FSF) are established in a single process step.
APCVD-SiO_x is used to prevent the p^+ emitter from being compensated during P diffusion. Its thickness needs to be adapted in order not to affect the p^+ profile during $POCl_3$ diffusion while keeping it removable.
For rear junction solar cells, it is crucial to ensure low recombination activity at the front. Therefore, a selectively etched-back FSF is to be established in the solar cell. An adjusted etch-back solution increases n^+ R_{sheet} successively and well controllably, accompanied by a drastic j_{0FSF} reduction while simultaneously almost completely maintaining p^+ R_{sheet}. A 43 Ω/sq APCVD-AlO_x passivated p^+ emitter achieves j_{0E} of only 52 fA/cm^2. Total *implied* V_{OC} of a pseudo solar cell structure attains up to 695 mV.
The newly developed APCVD p^+ emitter combined with the co-diffused and selectively etched-back FSF employed in an industrial n-type solar cell achieves 18.8% efficiency in a first experiment being still limited by a poor Ag/Al contact to the B-emitter.
Keywords: n-type, Boron, APCVD, Industrial, Selective

1 INTRODUCTION

Enhancing the energy conversion efficiency of solar cells is a fundamental approach to lower the cost of photovoltaic power. In this regard, n-type Si based devices have been proven to be a promising candidate, not only since record efficiencies above 25% have been attained by several manufactures recently [1-3]. Thus it is not surprising that the market share of n-type Si materials is expected to increase from today's <10% to ~40% within the next ten years [4]. The higher tolerance of minority carrier lifetime to common impurities and the performance not suffering B-O complex related light-induced degradation allow such ultra-high efficiencies.

To benefit from these n-type Si bulk characteristics, an industrially applicable technology to create a low recombinative and well contactable p^+ emitter is crucial. The p-n junction of n-type solar cells is frequently established by incorporation of B atoms into the Si wafer. The most common implementation is thermal diffusion of B from a liquid BBr_3 source [5].

An elegant alternative is the deposition of a capped B-doped silicon oxide layer (BSG), e.g. by plasma-enhanced chemical vapor deposition (PECVD) [6] or atmospheric pressure chemical vapor deposition (APCVD) [7,8]. By driving the B atoms into the Si wafer surface in a $POCl_3$ diffusion tube and a subsequent $POCl_3$ diffusion, p^+ emitter and n^+ back or front surface field (BSF/FSF) are established in a single process step, named co-diffusion. Furthermore, the separation of BSG deposition and drive-in step allows a structured doping source needed for local emitters in advanced solar cell concepts, such as the interdigitated back contact (IBC) cell.

Contrary to PECVD-BSG, the application of the doped layer including its capping by means of APCVD requires no vacuum and can hence be more cost-efficient. Thus, B-emitters created by APCVD can enable n-type solar cells to be industrially produced.

In the pursued cell concept, the B-emitter is located at the rear, ensuing several requirements and benefits:

- The B-emitter surface needs not be textured, leading to generally lower emitter saturation current densities j_{0E} due to a smaller crystal surface (e.g. [9]).
- For rear junction solar cells, it is crucial to ensure low recombination activity at the front. Therefore, a selectively etched-back FSF is to be established in the solar cell aiming at a j_{0FSF} being even smaller than j_{0E}.
- Since FSF and Si base have the same polarity, generally higher fill factors can be attained.
- For front side metalization, the established Ag screen-print (small finger width, high conductivity, low contact resistivity) can be used.
- The metalization at the rear can be performed by full-area Al (e.g. PVD or screen-print) with local contacts as an alternative to Ag/Al screen-printed paste known to cause shunts of the p-n junction [10,11].

2 EXPERIMENTAL

As preparative study prior to their integration into the solar cell process (Fig. 1), the creation of the APCVD boron emitter along with the co-diffused and selectively etched-back phosphorous FSF is investigated.

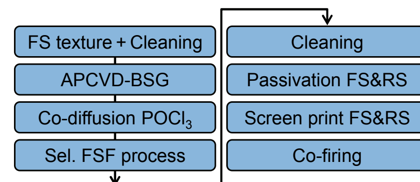

Figure 1: Processing scheme for an industrial n-type solar cell with APCVD B-rear emitter, co-diffused selective P-FSF, and screen-printed contacts.

In order to prevent the p^+ doped layer from being at least partly electrically compensated by the $POCl_3$ diffusion, the BSG is capped by undoped SiO_x, both

deposited by an inline belt APCVD tool from SCHMID Thermal Systems, Inc. featuring three injectors. The capping layer ought to be thin to facilitate its removal after the high temperature annealing, but does then require being thick enough to prevent P atoms from diffusing into the B-emitter.

During the FSF etch-back process [12], the boron rich layer (BRL) on top of the rear p^+ emitter, which forms during co-diffusion, is removed in the HF/HNO_3 etch-back solution. The composition of this solution has to be adjusted to the BRL thickness of the respective emitter and the desired etch-back depth of the FSF, aiming at a preferably small increase of emitter sheet resistance R_{sheet} during this process step.

In order to ensure very low saturation current density, two possible surface passivation schemes can be integrated into the solar cell process with reasonable additional effort:

- APCVD aluminum oxide (AlO_x) with capping PECVD-SiN_x for the rear B-emitter and PECVD-SiN_x front side passivation.
- A stack of thermal SiO_2 and PECVD-SiN_x passivating both sides of the solar cell.

Since metalization of the solar cells in this study is generated by screen-printed contacts, the aforementioned passivation stacks are characterized in the fired state.

All samples are subjected to a standard RCA cleaning before the BSG deposition. After co-diffusion in a $POCl_3$ tube furnace, the capping and BSG layers are removed in diluted HF. Prior to thermal oxidation or AlO_x APCVD, the wafers are RCA cleaned.

2.1 R_{sheet} and j_0 investigation

R_{sheet} of the n^+ and p^+ layers is measured by the four-point probe method and therefore on substrates with the respective opposite doping type (struc. 1&3 in Fig. 2).

j_0 is determined using 10 Ωcm Cz Si substrates (135 µm thick) with an alkaline-etched surface and the respective doped layer on both sides (struc. 2&3 in Fig. 2). For j_0 and *implied* V_{OC} measurement of a structure similar to the solar cell, the n^+ layer is applied at the front, the p^+ layer at the rear (struc. 4 in Fig. 2).

Figure 2: Sample structures for R_{sheet} and j_0 investigation of p^+ emitter and n^+ FSF.

j_0 and *implied* V_{OC} are determined from photoconductance decay measurement evaluated at an injection level of $\Delta n = 3\times10^{15}$ cm^{-3} (high level injection mode) [13] using a Sinton lifetime tester.

Since sample type 1 and 2 are simultaneously subjected to the etch-back process, the j_0 values can be assigned to the respective R_{sheet}.

2.2 n-type solar cells

The newly developed APCVD boron emitter combined with the co-diffused and selectively etched-back phosphorous FSF is then employed in an industrial bifacial n-type solar cell (Fig. 3) according to the processing sequence shown in Fig 1.

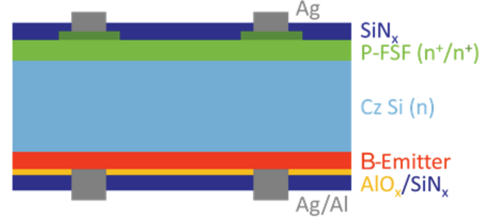

Figure 3: Industrial n-type bifacial solar cell with APCVD B-emitter (AlO_x/SiN_x passivation) and selective FSF (SiN_x passivation).

3 RESULTS & DISCUSSION

3.1 Co-diffused APCVD boron emitter

Varying capping layer thickness reveals a growing R_{sheet} increase of the p^+ emitter after $POCl_3$ diffusion with decreasing capping thickness (Fig. 4). Furthermore, a thinner capping layer yields significantly higher j_{0E} values (Fig. 4).

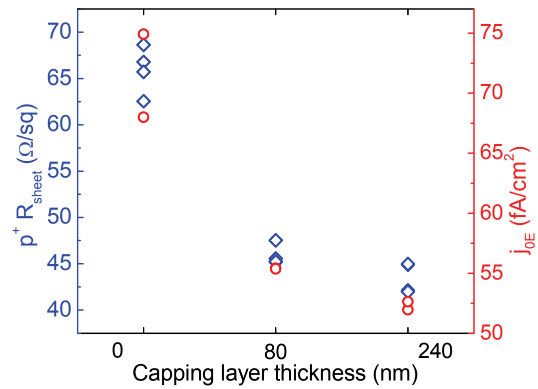

Figure 4: R_{sheet} and j_{0E} of a p^+ emitter (passivation by annealed AlO_x) after co-diffusion in a $POCl_3$ diffusion tube for different capping layer thicknesses.

ECV profiles of the B-emitters exhibit net surface doping concentrations which increase with capping layer thickness. Also, the B profiles feature a larger depth.

All findings can be explained by an increasing amount of P atoms with decreasing capping thickness which diffuse through the capping layer into the emitter, enhance recombination there, and derogate net p^+ doping.

An adjusted etch-back solution raises R_{sheet} of the FSF successively and well controllably while almost completely maintaining R_{sheet} of the emitter at the rear (Fig. 5). Firstly, this results from the different etching efficacy of p and n-doped layers [9]. Furthermore, R_{sheet} of the p^+ layer initially increases scarcely due to its relatively constant doping concentration and the absence of the kink and tail shape.

In order to examine a potential influence of the initial high temperature (>900°C) B drive-in upon the n^+ layer due to residual P atoms in the $POCl_3$ tube, two sample types are processed with the FSF created by the complete B drive-in + $POCl_3$ diffusion process and by the $POCl_3$ diffusion only (Fig. 5).

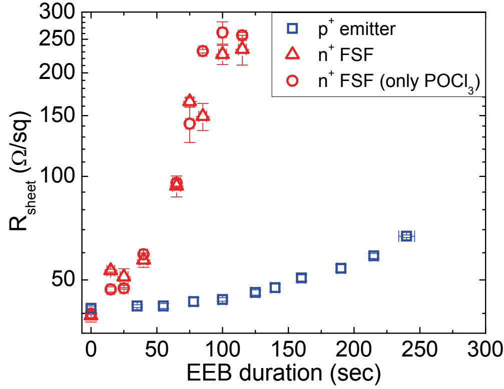

Figure 5: R_{sheet} of p^+ emitter and n^+ FSF after different etching durations in an adjusted etch-back solution. The FSF is created by the complete B drive-in + $POCl_3$ diffusion process and by a $POCl_3$ diffusion only.

Along with the increased FSF R_{sheet} during the etch-back, j_{0FSF} is reduced drastically (Fig. 6) as intended therewith. Especially for $R_{sheet} \leq 100$ Ω/sq, j_{0FSF} is further reduced (30-50 fA/cm^2) by enhancing passivation with a SiO_2/SiN_x stack instead of a single SiN_x layer (Fig. 6).

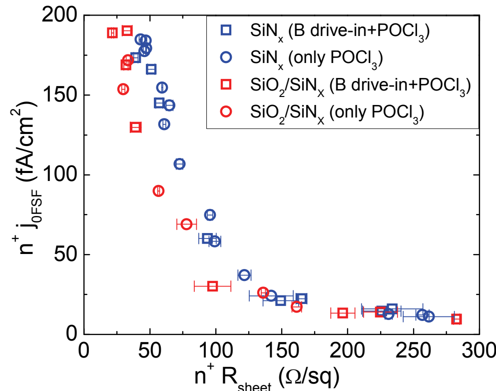

Figure 6: j_{0FSF} of the n^+ layer for different etch-back depths and passivation stacks. The FSF is created by the complete B drive-in + $POCl_3$ diffusion process and by a $POCl_3$ diffusion only.

The corresponding effective carrier lifetimes measured on sample structure 2 reach values of up to ~800 µs (B drive-in + $POCl_3$) or ~1200 µs ($POCl_3$ only), respectively. This can be regarded as the lower bound of the base carrier lifetime indicating that the Si substrate material is not considerably impaired by the high temperature processes in the $POCl_3$ diffusion tube.

At the same time, j_{0E} of the p^+ emitter remains virtually constant with increasing etch-back depth after an initial steep decrease by ~30 fA/cm^2 (Fig. 7). This drop may be caused by the removal of the BRL, which otherwise shields the actual emitter surface from being passivated. The more or less constant j_{0E} behavior is in correlation with the moderate ascent of emitter R_{sheet} during etch-back (cf. Fig. 5). A passivation consisting of SiO_2/SiN_x instead of APCVD-AlO_x capped by SiN_x further reduces j_{0E} by ~50 fA/cm^2. Besides a possible better passivating quality of SiO_2, this may be caused by a variation of the emitter doping profile, i.e. a reduction of surface doping density during high temperature thermal oxidation yielding less recombination.

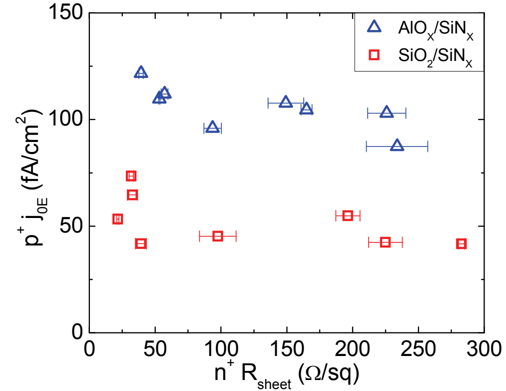

Figure 7: j_{0E} of the p^+ layer for different n^+ FSF etch-back depths and passivation stacks.

However, a higher passivation quality of the fired AlO_x/SiN_x stack is expected from optimizing co-firing parameters, since a 43 Ω/sq p^+ emitter passivated by annealed APCVD-AlO_x achieves a j_{0E} of only 52 fA/cm^2 (cf. Fig. 4, see also sec. 3.2). Moreover, using AlO_x instead of SiO_2 as passivation of the p^+ layer is beneficial because it can be deposited in the same industrial-type inline APCVD tool as employed for BSG deposition. Contrary to thermal oxidation, RCA pre-clean may be substituted, for instance, by less costly ozone cleaning.

Asymmetric j_0 samples featuring a structure similar to the final solar cell (struc. 4 in Fig. 2) yield j_{0p+n} values saturating for a FSF etched-back to ≳100 Ω/sq at about ~60 fA/cm^2 (Fig. 8). j_{0p+n} of the $AlO_x/SiN_x – SiN_x$ passivated samples is not consistent with the addition of j_{0E} (Fig. 7) and j_{0FSF} (Fig. 6), since measurement uncertainty for high j_0 values is greater.

Additionally determined *implied* V_{OC} of the same samples indicate the potential of the solar cell. The SiO_2/SiN_x passivated samples attain values of up to 695 mV.

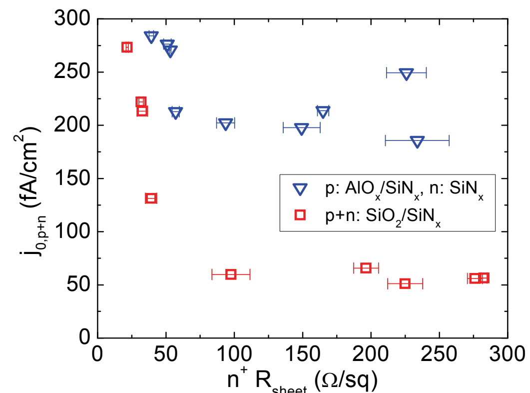

Figure 8: j_{0p+n} of solar cell similar structures for different etch-back depths and combinations of passivation stacks.

3.2 n-type solar cells

As a proof of concept, initial bifacial n-type solar cells (cf. Fig. 3) are manufactured employing a ~70 Ω/sq B-emitter. In Tab. I, the IV characteristics of the best solar cells with $AlO_x/SiN_x – SiN_x$ or $SiO_2/SiN_x – SiO_2/SiN_x$ passivation scheme, respectively, are compared.

Table I: IV characteristics of the best bifacial n-type solar cells featuring $AlO_x/SiN_x – SiN_x$ or $SiO_2/SiN_x – SiO_2/SiN_x$ passivation scheme.

	V_{OC} (mV)	j_{SC} (mA/cm^2)	*FF* (%)	η (%)
AlO_x/SiN_x – SiN_x	655	38.5	73.9	18.6
SiO_2/SiN_x – SiO_2/SiN_x	647	38.4	75.8	18.8

V_{OC} of the SiO_2/SiN_x passivated solar cell is 8 mV lower whereas *FF* is ~2%$_{abs}$ higher. Correspondingly, specific contact resistivity of the Ag/Al contact to the B-emitter with SiO_2/SiN_x passivation is reduced by 9 mΩcm^2 yielding a series resistance decrease by 0.6 Ωcm^2 compared to the AlO_x/SiN_x passivation.

Optimal firing temperature of the solar cells with SiO_2/SiN_x passivation is ~40 K higher. *Implied* V_{OC} values of comparable pseudo solar cells without metalization exhibit their maxima (677 mV for AlO_x/SiN_x, 675 mV for SiO_2/SiN_x) each at the same firing temperature as the solar cells indicating AlO_x to be less firing stable. Furthermore, the SiO_2/SiN_x passivated solar cells feature a ~0.1 µm deeper emitter profile (due to the additional high temperature oxidation) which is less susceptible to shunting by Al spikes and may also account for the better contact [14]. Nevertheless, the higher firing temperatures impair passivation quality more heavily.

4 CONCLUSION & OUTLOOK

In order to prevent a p$^+$ emitter from APCVD-BSG from being compensated by P in a $POCl_3$ co-diffusion, a SiO_x capping layer is deposited also by APCVD. The p$^+$ R_{sheet} increase after $POCl_3$ co-diffusion is more pronounced with diminishing capping layer thickness while j_{0E} increases significantly because more P atoms derogate net p$^+$ doping of the B-emitter.

For rear junction solar cells, it is crucial to ensure low recombination activity at the front. Therefore, a selectively etched-back FSF is to be established in the solar cell. An adjusted etch-back solution increases n$^+$ R_{sheet} successively and well controllably, accompanied by a drastic j_{0FSF} reduction, while simultaneously almost completely maintaining p$^+$ R_{sheet} at the rear.

No considerable Si substrate impairment due to the high temperature processes in the $POCl_3$ diffusion tube could be ascertained. A 43 Ω/sq APCVD-AlO_x passivated p$^+$ emitter achieves a j_{0E} of 52 fA/cm^2. Total *implied* V_{OC} of a pseudo solar cell structure attains up to 695 mV.

The newly developed APCVD p$^+$ emitter combined with the co-diffused and selectively etched-back FSF has been employed in industrial bifacial n-type solar cells. Efficiencies of up to 18.8% have been attained, mainly limited by a poor Ag/Al contact to the B-emitter.

Further investigations are aimed at reducing contact resistivity and the *implied* V_{OC} to V_{OC} discrepancy by the appropriate adaption of the B-emitter profile.

5 ACKNOWLEDGEMENTS

The authors would like to thank Florian Mutter for processing assistance. Part of this work was financially supported by the German Federal Ministry for the Environment, Nature Conservation and Nuclear Safety (FKZ 0325581) and within the “PARADIES” project (FKZ 0325632). The content is the responsibility of the authors.

6 REFERENCES

[1] D.D. Smith, P. Cousins, S. Westerberg, R. De Jesus-Tabajonda, G. Aniero, Y.-C. Shen, Proc. 40th IEEE PVSC (2014) 601, in print.

[2] J. Nakamura, N. Asano, T. Hieda, C. Okamoto, T. Ohnishi, M. Kobayashi, H. Tadokoro, R. Suganuma, Y. Matsumoto, H. Katayama, K. Higashi, T. Kamikawa, K. Kimoto, M. Harada, T. Sakai, H. Shigeta, T. Kuniyoshi, K. Tsujino, L. Zou, N. Koide, K. Nakamura, Proc. 40th IEEE PVSC (2014) 283, in print.

[3] K. Masuko, M. Shigematsu, T. Hashiguchi, D. Fujishima, M. Kai, N. Yoshimura, T. Yamaguchi, Y. Ichihashi, T. Mishima, N. Matsubara, T. Yamanishi, T. Takahama, M. Taguchi, E. Maruyama, S. Okamoto, Proc. 40th IEEE PVSC (2014) 191, in print.

[4] International Technology Roadmap for Photovoltaic (ITRPV), 5th Edition, 2013 Results (2014).

[5] Y. Schiele, S. Fahr, S. Joos, G. Hahn, B. Terheiden, Proc. 28th EU PVSEC (2013) 1242.

[6] B. Bazer-Bachi, C. Oliver, B. Semmache, Y. Pellegrin, M. Gauthier, N. Le Quang, M. Lemiti, Proc. 26th EU PVSEC (2011) 1155.

[7] L.D. Bartholomew, N.M. Gralenski, J.C. Sisson, G.U. Pignatel, Eur. T. Telecommun. 1 (1990) 167.

[8] P. Rothhardt, C. Demberger, A. Wolf, D. Biro, En. Proc. 38 (2013) 305.

[9] Y. Schiele, S. Joos, G. Hahn, B. Terheiden, En. Proc. (2014), in print.

[10] R. Lago, L. Pérez, H. Kerp, I. Freire, I. Hoces, N. Azkona, F. Recart, J.C. Jimeno, Prog. Photovoltaics: Res. Appl. 18 (2010) 20.

[11] A. Frey, J. Engelhardt, S. Fritz, S. Gloger, G. Hahn, B. Terheiden, 2DO.4.5, this conference (2014).

[12] H. Haverkamp, A. Dastgheib-Shirazi, B. Raabe, F. Book, G. Hahn, Proc. 33rd IEEE PVSC (2008) 430.

[13] D.E. Kane, R.M. Swanson, Proc. 18th IEEE PVSC (1985) 578.

[14] Y. Schiele, G. Hahn, B. Terheiden, 2AV.2.5, this conference (2014).